

Absence of the enhanced intra-4*f* transition cross section at 1.5 μm of Er^{3+} in Si-rich SiO_2

H. Mertens^{a)} and A. Polman

Center for Nanophotonics, FOM Institute for Atomic and Molecular Physics, Kruislaan 407, 1098 SJ Amsterdam, The Netherlands

I. M. P. Aarts, W. M. M. Kessels, and M. C. M. van de Sanden

Department of Applied Physics, Eindhoven University of Technology, P.O. Box 513, 5600 MB Eindhoven, The Netherlands

(Received 4 October 2004; accepted 11 May 2005; published online 8 June 2005)

We present measurements of the optical absorption cross section of the ${}^4I_{15/2} \rightarrow {}^4I_{13/2}$ transition at 1.5 μm of Er^{3+} ions embedded in SiO_2 and Si-rich oxide, using cavity ringdown spectroscopy on thin films. The peak absorption cross section for Er^{3+} embedded in Si-rich oxide (10 at. % excess Si) was found to be $(8 \pm 2) \times 10^{-21} \text{ cm}^2$ at 1536 nm, similar to typical values for Er embedded in SiO_2 . The data imply that the silicon nanoclusters incorporated in Si-rich oxide do not enhance the peak cross section of the $\text{Er}^{3+} {}^4I_{15/2} - {}^4I_{13/2}$ transition by 1-2 orders of magnitude, contrary to what has been reported in earlier work. © 2005 American Institute of Physics. [DOI: 10.1063/1.1949720]

Erbium-doped Si-rich oxide (SRO:Er) is an optical gain medium in which Er^{3+} ions, exhibiting an intra-4*f* transition at 1.5 μm , are surrounded by silicon nanoclusters that serve as broadband sensitizers.¹⁻³ A sensitizer coupled to an Er^{3+} ion absorbs light at a cross section several orders of magnitude larger than Er, and then transfers its energy to the Er^{3+} ion. Sensitizers have the potential to enable optical amplification at 1.5 μm using low-cost light-emitting diodes in top-pumping configuration, instead of a waveguide-coupled laser tuned to an Er transition.

In addition to the sensitization effect, which is of great technological interest, it has been reported that silicon nanoclusters would enhance the absorption and emission cross sections of the ${}^4I_{15/2} - {}^4I_{13/2}$ transition at 1.5 μm of Er^{3+} embedded in SiO_2 by 1-2 orders of magnitude.^{4,5} This presumed enhancement was derived from optical absorption spectroscopy in linear waveguides,⁴ and it has been invoked to explain the high signal enhancement in SRO:Er linear amplifiers.⁵ The enhanced emission cross section has also been used as an input parameter in a model describing the gain characteristics of SRO:Er amplifiers.⁶

If true, the cross section enhancement would have a broad impact on Er amplifier and laser technology as it implies an enhancement of the optical gain coefficient by the same 1-2 orders of magnitude. Thus more compact devices would be possible using SRO:Er.

Both reported cross-section enhancements are based on indirect measurements, and a direct determination is still lacking. In this letter, we present measurements of the Er^{3+} absorption cross section in both SRO:Er and SiO_2 :Er by cavity ringdown spectroscopy (CRDS) on thin films,^{7,8} which is an approach that does not require estimates on the overlap between an optical mode and the erbium profile as in earlier work. From the data it is concluded that the earlier reported 1-2 orders of magnitude enhancement of the cross section of the $\text{Er}^{3+} {}^4I_{15/2} - {}^4I_{13/2}$ transition at 1.5 μm due to silicon nanoclusters is incorrect.

SRO:Er and SiO_2 :Er thin films were fabricated by ion implantation and thermal annealing of 2-mm-thick high-purity fused-silica substrates (Heraeus Suprasil[®] 300). In the first fabrication step, the substrates were implanted with 300- and 150-keV Er ions to a total fluence of $1.2 \times 10^{16} \text{ at/cm}^2$. The Er peak concentration measured by Rutherford back-scattering spectrometry was 2.3 at. %. Subsequently, a dual Si implant (73 and 30 keV) was applied to part of the Er-implanted samples to fabricate SRO:Er films. The Si fluences were chosen such that an excess Si concentration of ~ 10 at. % was achieved over the full Er depth profile. One of the SRO:Er samples was annealed at 800 °C for 30 min in flowing Ar and at 700 °C for 30 min in forming gas ($\text{H}_2:\text{N}_2$ at 1:9) to optimize the Er^{3+} 1.5 μm photoluminescence (PL) intensity.⁹ An SiO_2 :Er reference sample (i.e., without Si incorporation) was exposed to the same thermal treatment. A second SRO:Er sample was annealed at 1000 °C for 30 min in flowing Ar, comparable to the thermal treatments described in Refs. 4 and 5. PL excitation spectroscopy using different lines of an Ar^+ laser¹ showed that Er^{3+} embedded in SRO was mainly excited indirectly, confirming the coupling between Er^{3+} and silicon nanoclusters in these samples.

The Er^{3+} absorption spectrum at 1.5 μm was determined by CRDS on thin films, which is a direct and highly sensitive absorption measurement method in which the sample under investigation is placed inside a high quality optical cavity (see the inset of Fig. 1).^{7,8} The measurements were carried out with the tunable idler output of an optical parametric oscillator (OPO), which is pumped by the third harmonic of a pulsed Nd:YAG laser operating at 30 Hz. The idler output of the OPO was tuned over the wavelength range of 1450–1630 nm with an accuracy of 2 nm, and the resulting pulse had a typical bandwidth of 2 nm, a duration of 5 ns, and a pulse energy of 10 mJ. The pulse was injected into a stable optical cavity (length 0.4 m) formed by two planoconcave highly reflecting ($R > 0.9997$) mirrors without using mode-matching optics, resulting in an effective spot size of 3 mm. Thus, the total injected pulse energy was less than 3 μJ . The cavity was purged with dry nitrogen to reduce the effects of H_2O absorption lines. The temporal decrease in

^{a)}Electronic mail: mertens@amolf.nl

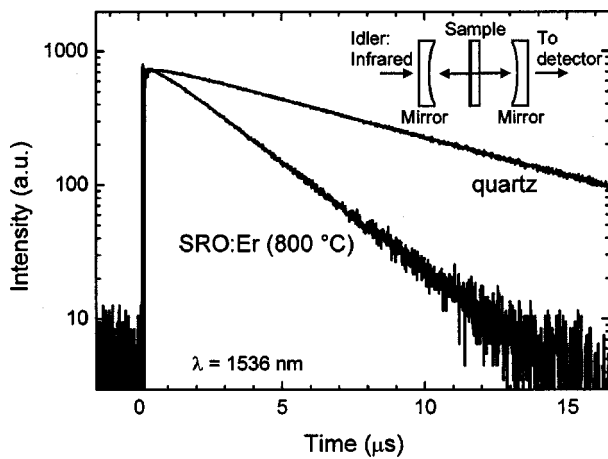


FIG. 1. Cavity ringdown transients for both an SRO:Er sample and a bare quartz substrate detected at 1536 nm upon injection of a 5 ns pulse at $t=0$. The experimental configuration is sketched in the inset.

light intensity inside the cavity upon pulse injection was detected with a photodiode. Individual transients were sampled using a 12 bit, 100 MHz data acquisition system.

Figure 1 shows cavity ringdown transients detected at 1536 nm for both an SRO:Er sample that was annealed at 800 °C and a bare quartz substrate. After the first microsecond, the transients exhibit a single-exponential behavior of which the rate is determined by the intrinsic cavity loss and the loss generated by the sample placed in the cavity.⁷ The ringdown time for SRO:Er (3 μ s) is significantly shorter than for quartz (8 μ s) due to the stronger extinction of the SRO:Er sample. The single-exponential parts of individual transients were fitted with a standard weighted linear regression technique to extract the ringdown time. Reported values of the optical loss per pass, which includes both scattering and absorption contributions, have been corrected for the empty cavity response and were deduced from averages of the ringdown time over 100 laser shots at every wavelength.

Figure 2 shows the optical loss spectra for SRO:Er and SiO₂:Er determined in this way. Every optical loss spectrum shows a characteristic Er³⁺ absorption spectrum superimposed on a background that is decreasing with wavelength,

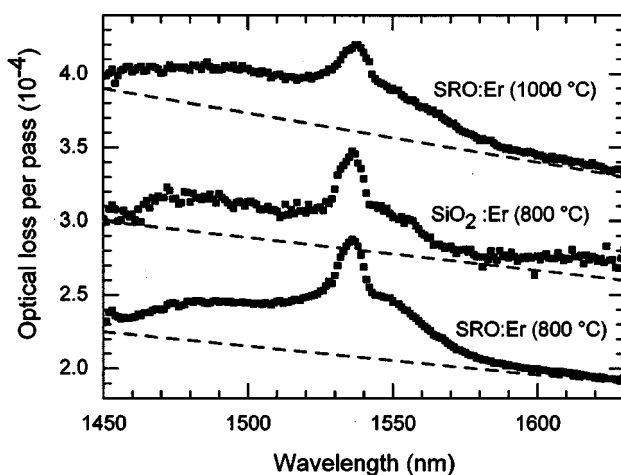


FIG. 2. Optical loss spectra for SRO:Er (annealed at 800 and 1000 °C) and SiO₂:Er (annealed at 800 °C) measured by CRDS on thin films. All spectra have been corrected for the empty cavity response. Estimates of the background loss are indicated for all spectra (dashed lines).

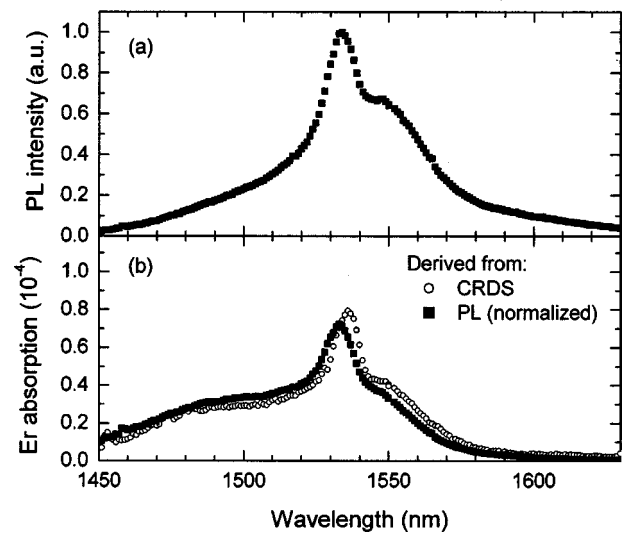


FIG. 3. (a) PL spectrum of SRO:Er (annealed at 800 °C) measured at room temperature under 488 nm excitation. (b) Er absorption spectra derived both from the optical loss spectrum, by a subtraction of the background (○), and from the PL spectrum by means of McCumber theory (■).

which is attributed to loss processes not related to Er such as scattering. Repeated measurements after sample realignment gave reproducible results for both peak shape and magnitude, as well as for the decreasing background trend, with some variations in background level. We attribute the latter to variations in both alignment and sample quality.

The estimates of the background losses indicated in Fig. 2 (dashed lines) are based on a qualitative comparison with absorption spectra derived by PL spectroscopy using McCumber theory,^{10,11} as is illustrated in Fig. 3. Figure 3(a) shows a PL spectrum for SRO:Er (annealed at 800 °C) taken at room temperature. The absorption spectral shape derived from this spectrum is shown in Fig. 3(b), together with the corresponding absorption spectrum derived from the optical loss data shown in Fig. 2 by subtraction of the background loss (dashed line). The spectral resemblance between the CRDS-based spectrum and the normalized PL-based spectrum validates the estimate of the background loss.

The important feature shown in Fig. 2 is that, for all three samples, the Er absorption is very similar over the entire wavelength range (within 20%). The Er³⁺ $^4I_{15/2} \rightarrow ^4I_{13/2}$ absorption cross section is thus found to be similar for SiO₂:Er and SRO:Er annealed at either 800 or 1000 °C. Here, it is assumed that all Er ions are in the 3+ valence state, which is justified by the fact that no other valences of Er are reported for a variety of hosts.¹² In addition, X-ray absorption spectroscopy of the Er $3d^{10}4f^{11} \rightarrow 3d^94f^{12}$ transitions for Er-doped silicon has shown no evidence of other Er valence states.¹³

The Er³⁺ $^4I_{15/2} \rightarrow ^4I_{13/2}$ absorption cross section for SRO:Er can directly be obtained from Fig. 3(b) by dividing the Er absorption by the Er areal density. This procedure yields a peak absorption cross section, which is related to the maximum gain coefficient for SRO:Er amplifiers, of $(8 \pm 2) \times 10^{-21}$ cm² at 1536 nm, where the error bar is determined mainly by the uncertainty in the background level of the absorption measured. This result is similar to typical values obtained for Er embedded in glasses:¹⁴ $(4.8 - 7.0) \times 10^{-21}$ cm², confirming that silicon nanoclusters do not enhance the cross section of the Er³⁺ $^4I_{15/2} \rightarrow ^4I_{13/2}$ transition by

1-2 orders of magnitude. Note that the cross section in SRO:Er is expected to be 10%–20% larger than in SiO₂:Er due to the higher refractive index of the heterogeneous SRO,¹⁵ but the limited signal-to-noise ratio of the SiO₂:Er sample does not allow one to resolve this difference from the performed measurements.

For the determination of the Er³⁺ $^4I_{15/2} \rightarrow ^4I_{13/2}$ absorption cross section, bleaching of the Er³⁺ ions has been neglected. This is legitimate since the effective pump power inside the cavity was adequately low, as can be derived in the following way. Upon pulse injection, the pulse energy in the cavity was lower than 3 μ J. Taking into account the cavity length, ringdown time, and laser spot size, this corresponds to an effective time-integrated photon flux of 6×10^{17} photons/cm² per pulse. This implies that for an Er³⁺ absorption cross section of 8×10^{-21} cm² less than 0.5% of the Er³⁺ population was inverted per pulse. Subsequent pulses can be regarded independently, since the interval between them (33 ms) is much larger than the Er³⁺ lifetime in our samples (\sim 3 ms). The relatively short Er³⁺ lifetime is ascribed to the presence of nonradiative de-excitation channels in the heavily doped matrix. If the cross section had been 2×10^{-19} cm², still only 12% of the Er³⁺ population would have been inverted, and the Er absorption peak would be 20 times larger than observed. This implies that the error in the absorption cross section induced by Er³⁺ bleaching is much smaller than the error induced by the uncertainty in the background level.

Finally, we speculate on the apparent discrepancy between the cross section for SRO:Er derived here, and the much larger values claimed in earlier work. Kik's tenfold enhanced cross-section claim⁴ was based on a calculation that involved an estimated overlap between the optical waveguide mode and the Er profile. Possibly, this overlap was underestimated. As CRDS does not require estimates on modal overlap in order to determine the absorption cross section, the method presented in the current work provides more reliable results. The reported near-hundredfold cross section enhancement derived from gain characteristics of SRO:Er linear amplifiers by Han *et al.*⁵ remains puzzling. In any case, such an enhancement is inconsistent with the Er luminescence lifetime of 8 ms reported in the same paper: according to the Füchtbauer-Ladenburg equation,¹¹ the reported Er emission cross section of $(2 \pm 0.5) \times 10^{-19}$ cm²

would correspond to a radiative lifetime of \sim 0.3 ms.

In conclusion, we have measured the optical absorption cross section of the Er³⁺ $^4I_{15/2} - ^4I_{13/2}$ transition at 1.5 μ m in both SRO:Er and SiO₂:Er by cavity ringdown spectroscopy on thin films, proving that this is a suitable technique for the determination of rare-earth absorption cross sections. The peak absorption cross section for SRO:Er was found to be $(8 \pm 2) \times 10^{-21}$ cm², which is identical (within 20%) to the measured cross section for SiO₂:Er, and which is a typical value for Er embedded in glasses. This result is in disagreement with earlier reported cross sections enhancements for SRO:Er. The conclusion affects modeling of the gain characteristics of SRO:Er materials that use the presumed enhanced cross section as an input parameter.⁶

The authors would like to thank Bram Hoex for assistance with part of the cavity ringdown measurements, and Jan van der Elsken and Jeroen Goedkoop for many useful discussions. This work is part of the research program of the "Stichting voor Fundamenteel Onderzoek der Materie (FOM)," which is financially supported by the "Nederlandse organisatie voor Wetenschappelijk Onderzoek (NWO)."

¹S. Lombardo, S. U. Campisano, G. N. van den Hoven, A. Cacciato, and A. Polman, Appl. Phys. Lett. **63**, 1942 (1993).

²M. Fujii, M. Yoshida, Y. Kanzawa, S. Hayashi, and K. Yamamoto, Appl. Phys. Lett. **71**, 1198 (1997).

³G. Franzò, D. Pacifici, V. Vinciguerra, F. Priolo, and F. Iacona, Appl. Phys. Lett. **76**, 2167 (2000).

⁴P. G. Kik and A. Polman, J. Appl. Phys. **91**, 534 (2002).

⁵H.-S. Han, S.-Y. Seo, J. H. Shin, and N. Park, Appl. Phys. Lett. **81**, 3720 (2002).

⁶D. Pacifici, G. Franzò, F. Priolo, F. Iacona, and L. Dal Negro, Phys. Rev. B **67**, 245301 (2003).

⁷G. Berden, R. Peeters, and G. Meijer, Int. Rev. Phys. Chem. **19**, 565 (2000).

⁸T. M. P. Aarts, B. Hoex, A. H. M. Smets, R. Engeln, W. M. M. Kessels, and M. C. M. van de Sanden, Appl. Phys. Lett. **84**, 3079 (2004).

⁹G. Franzò, S. Boninelli, D. Pacifici, F. Priolo, F. Iacona, and C. Bongiorno, Appl. Phys. Lett. **82**, 3871 (2003).

¹⁰D. E. McCumber, Phys. Rev. **136**, A954 (1964).

¹¹W. J. Miniscalco and R. S. Quimby, Opt. Lett. **16**, 258 (1991).

¹²J. Röhler, in *Handbook on the Physics and Chemistry of Rare Earths*, edited by K. A. Gschneider, Jr., L. Eyring, and S. Hüfner (North-Holland, Amsterdam, 1987), Vol. 10, Chap. 71.

¹³J. B. Goedkoop and A. Polman (unpublished).

¹⁴W. J. Miniscalco, J. Lightwave Technol. **9**, 234 (1991).

¹⁵E. Snoeks, A. Lagendijk, and A. Polman, Phys. Rev. Lett. **74**, 2459 (1995).